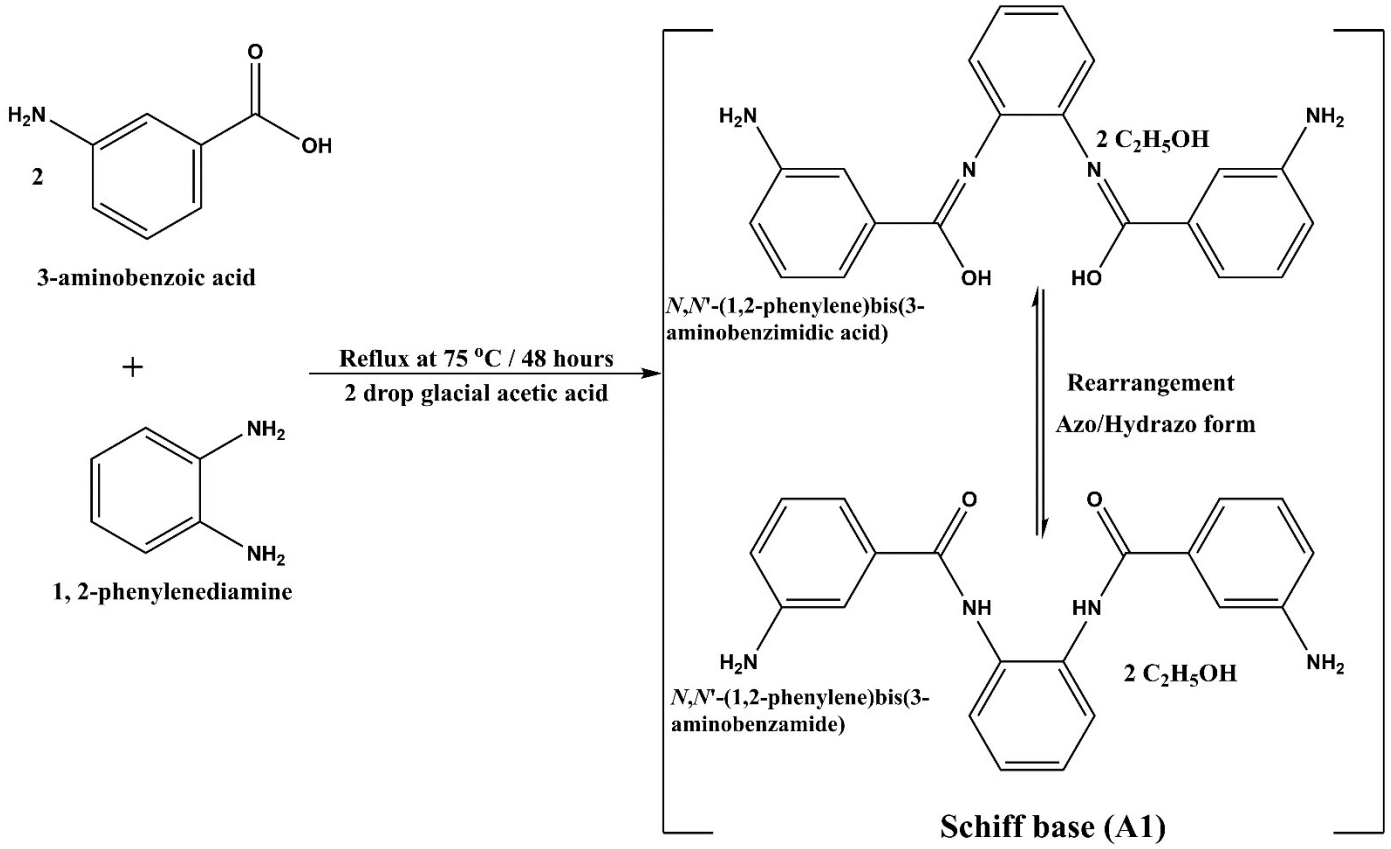

Fig. S1: The proposed mechanism of the Schiff base ligand **(A1)** synthesis Scheme.

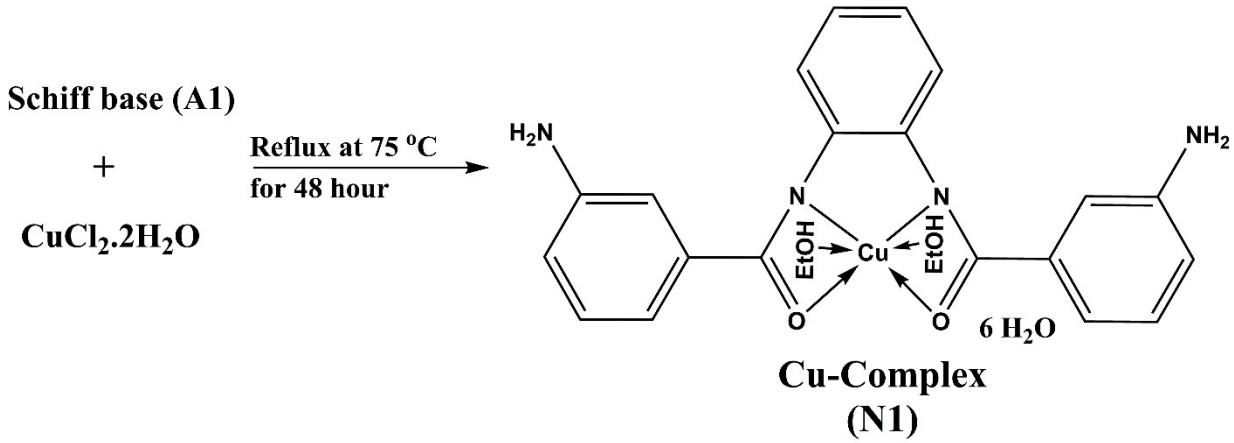

Fig. S2: The proposed mechanism of the nano copper complex **(N1)** synthesis Scheme.

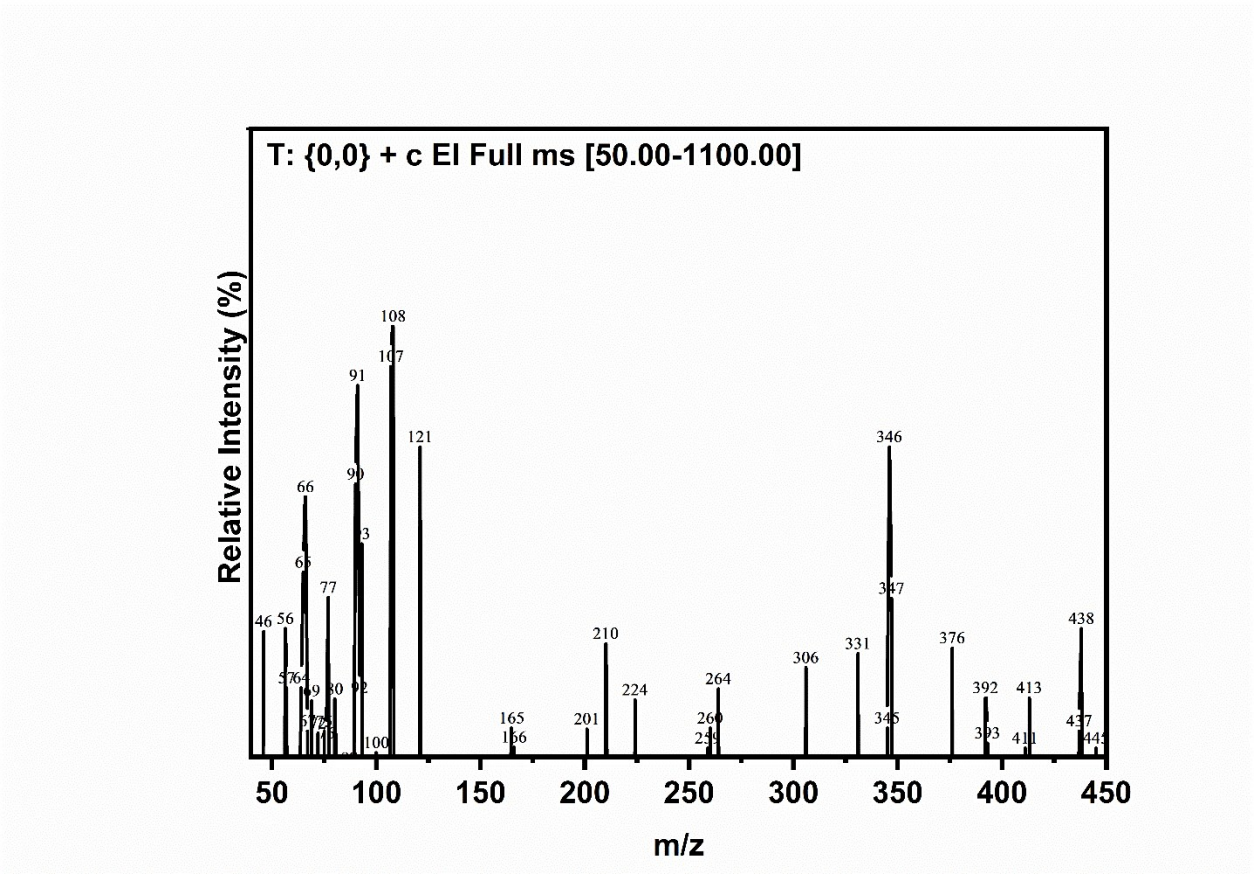

Fig. S3: The mass spectrum of the Schiff base ligand **(A1)**.

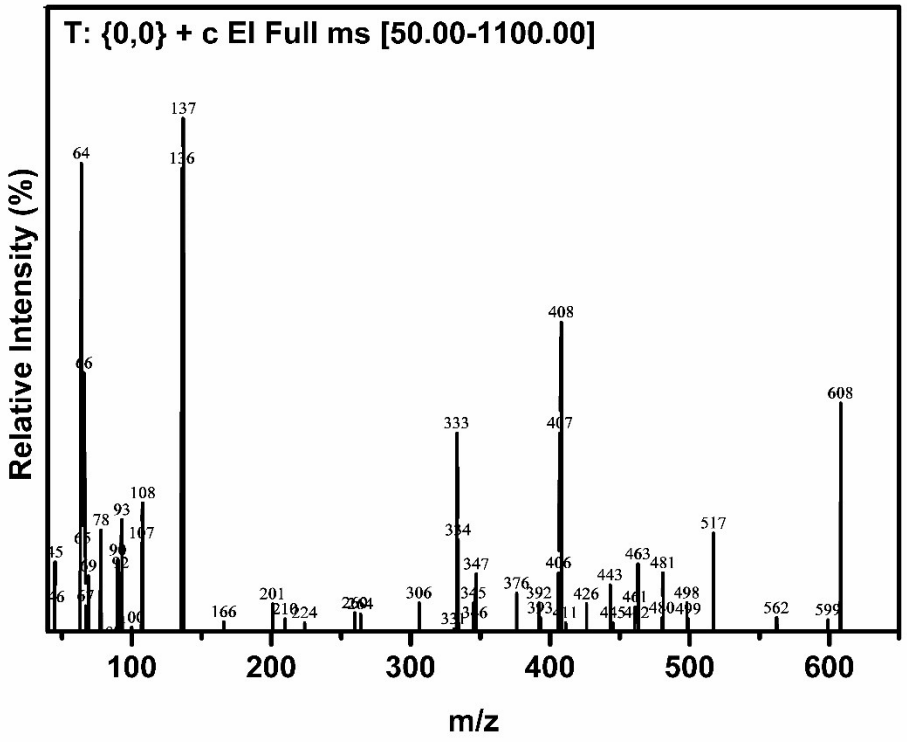

Fig. S4: The mass spectrum of the nano copper complex **(N1)**.

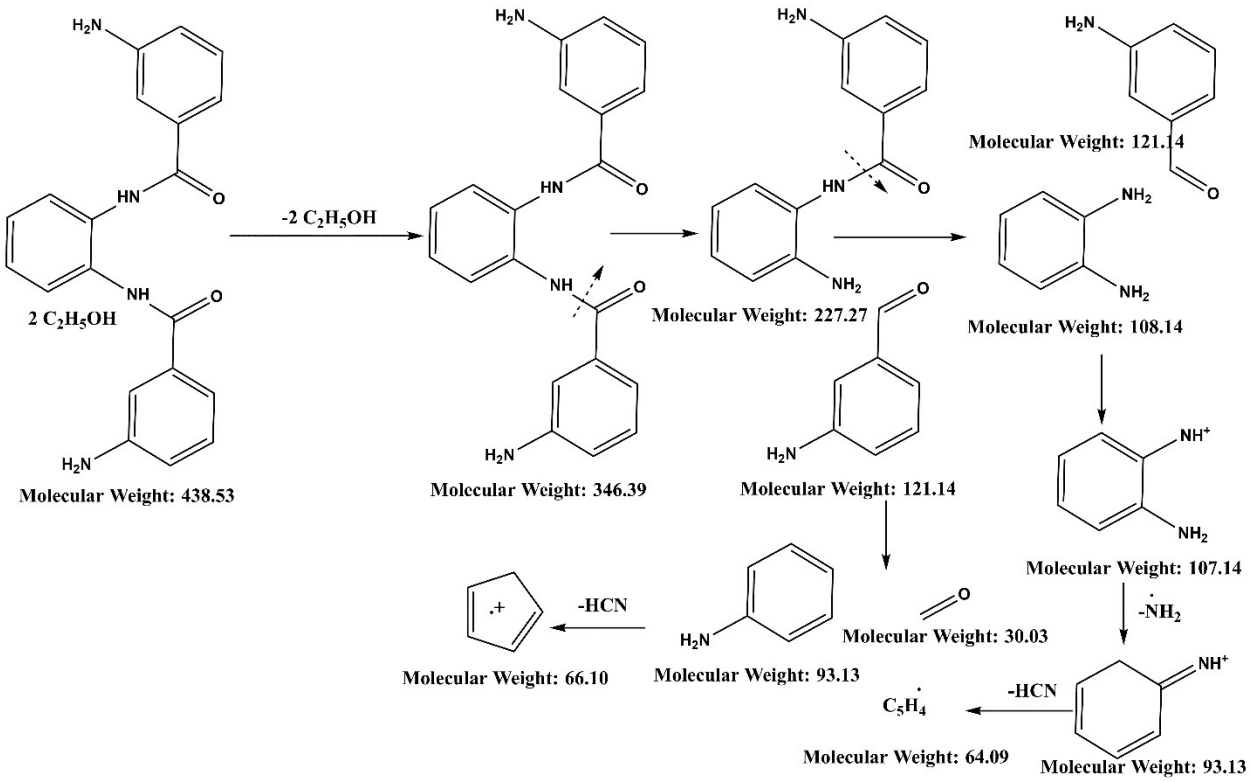

Fig. S5: The proposed fragmentation Scheme of the Schiff base ligand **(A1)**.

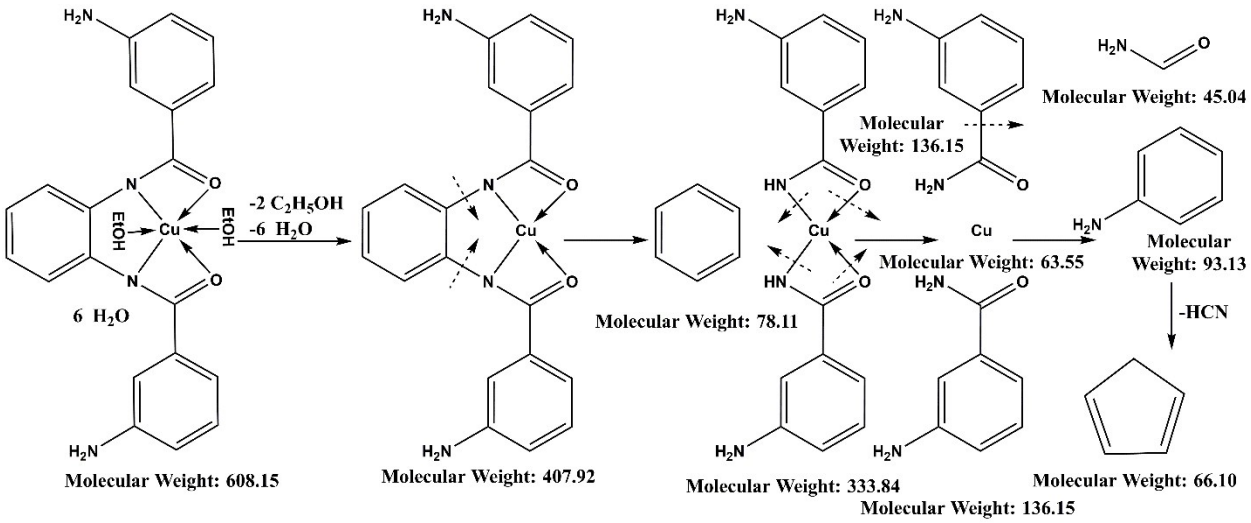

Fig. S6: The proposed fragmentation Scheme of the nano copper complex **(N1)**.

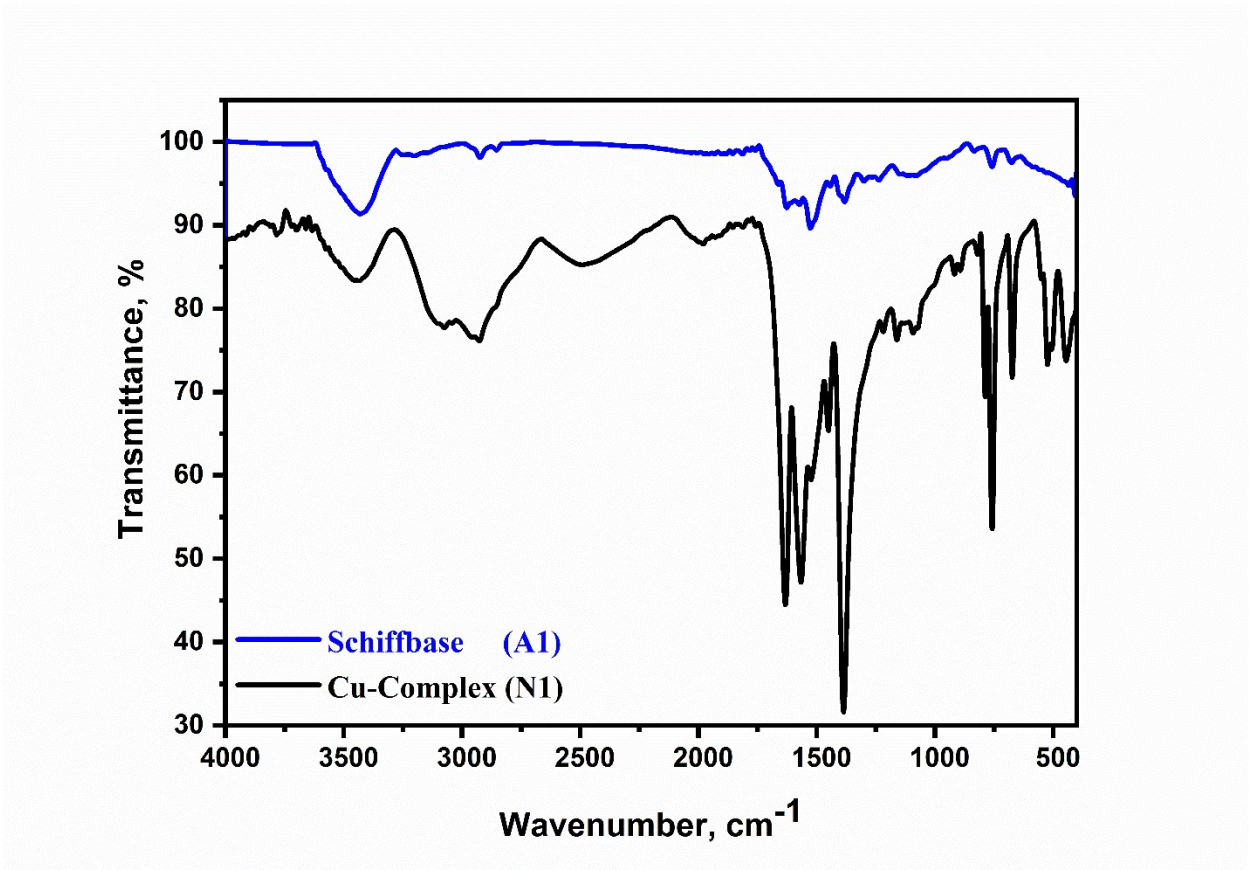

Fig. S7: The FT-IR spectrum of the Schiff base ligand **(A1)** and nano copper complex **(N1)**.

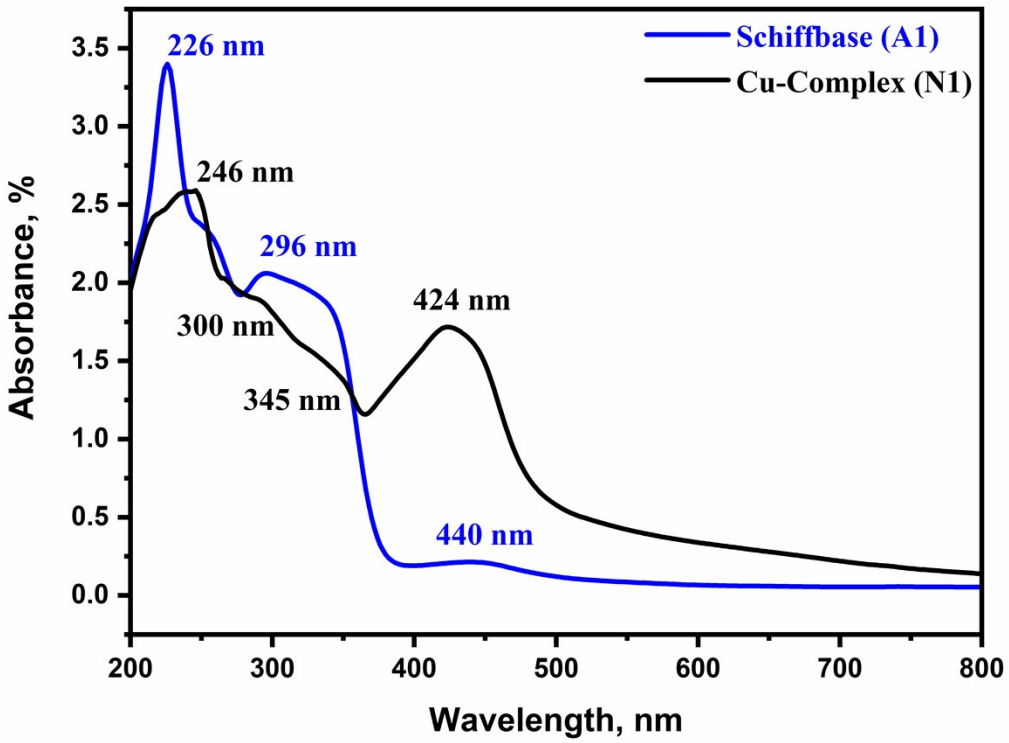

Fig. S8: The electronic absorption spectra of Schiff base ligand **(A1)** and nano copper complex **(N1)**.

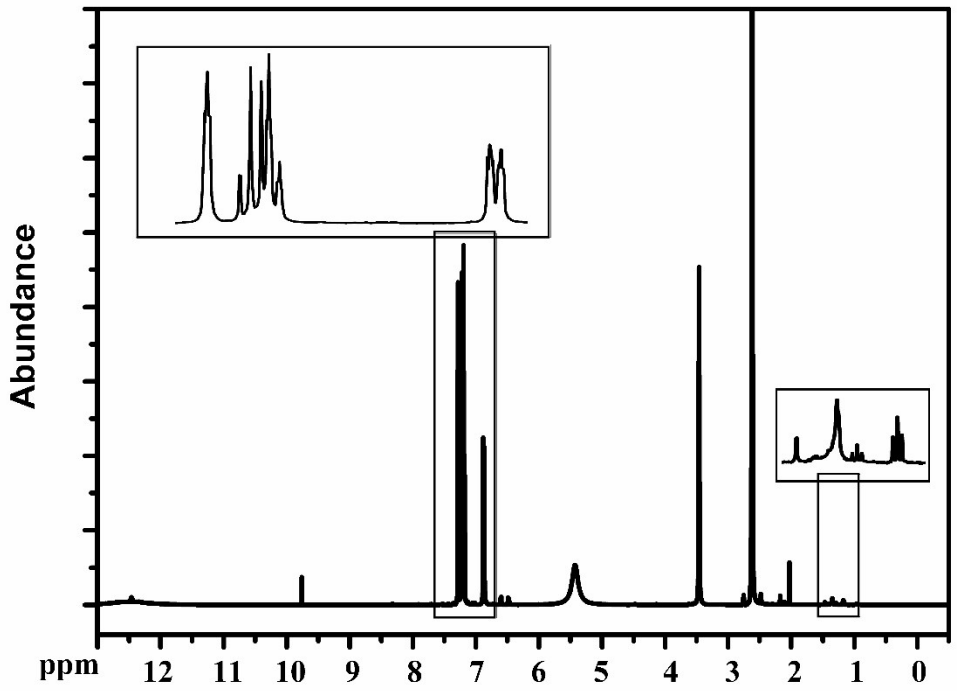

Fig. S9: The ^{1}H-NMR spectrum of Schiff base ligand **(A1)**.

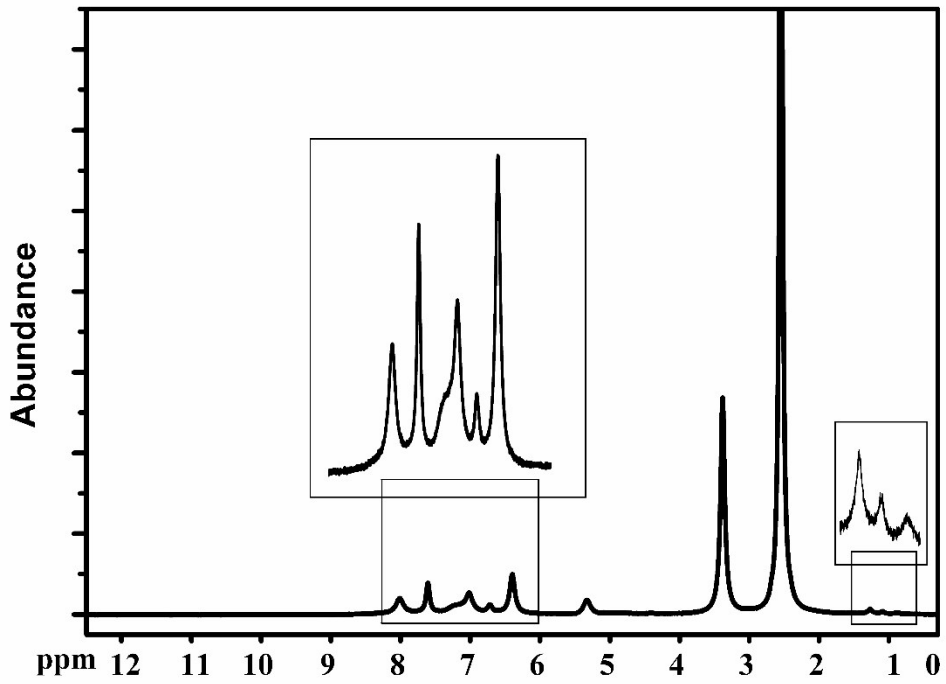

Fig. S10: The ^{1}H-NMR spectrum of nano copper complex **(N1)**.

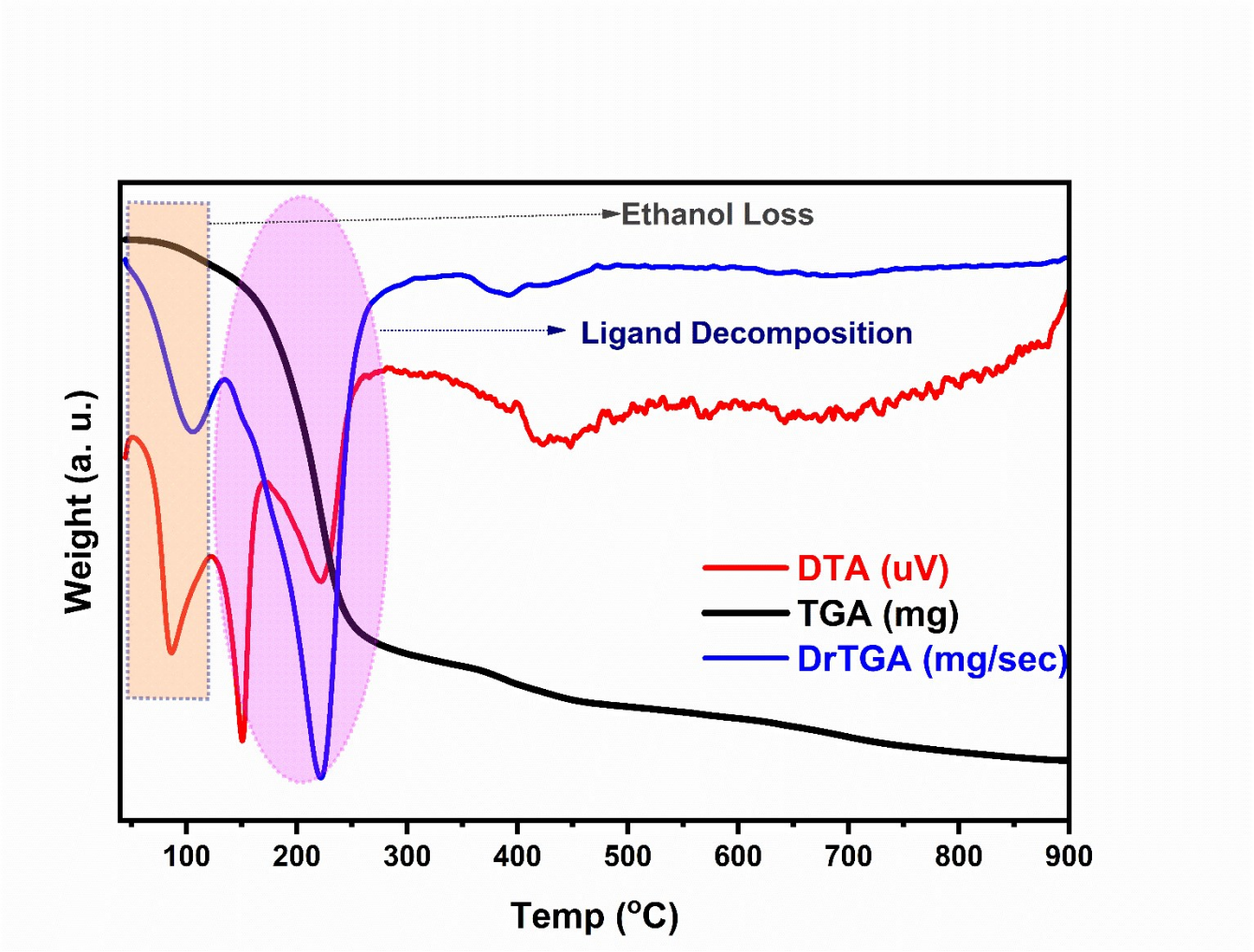

Fig. S11: The thermogravimetric analysis (TGA-DTGA) of the A1.

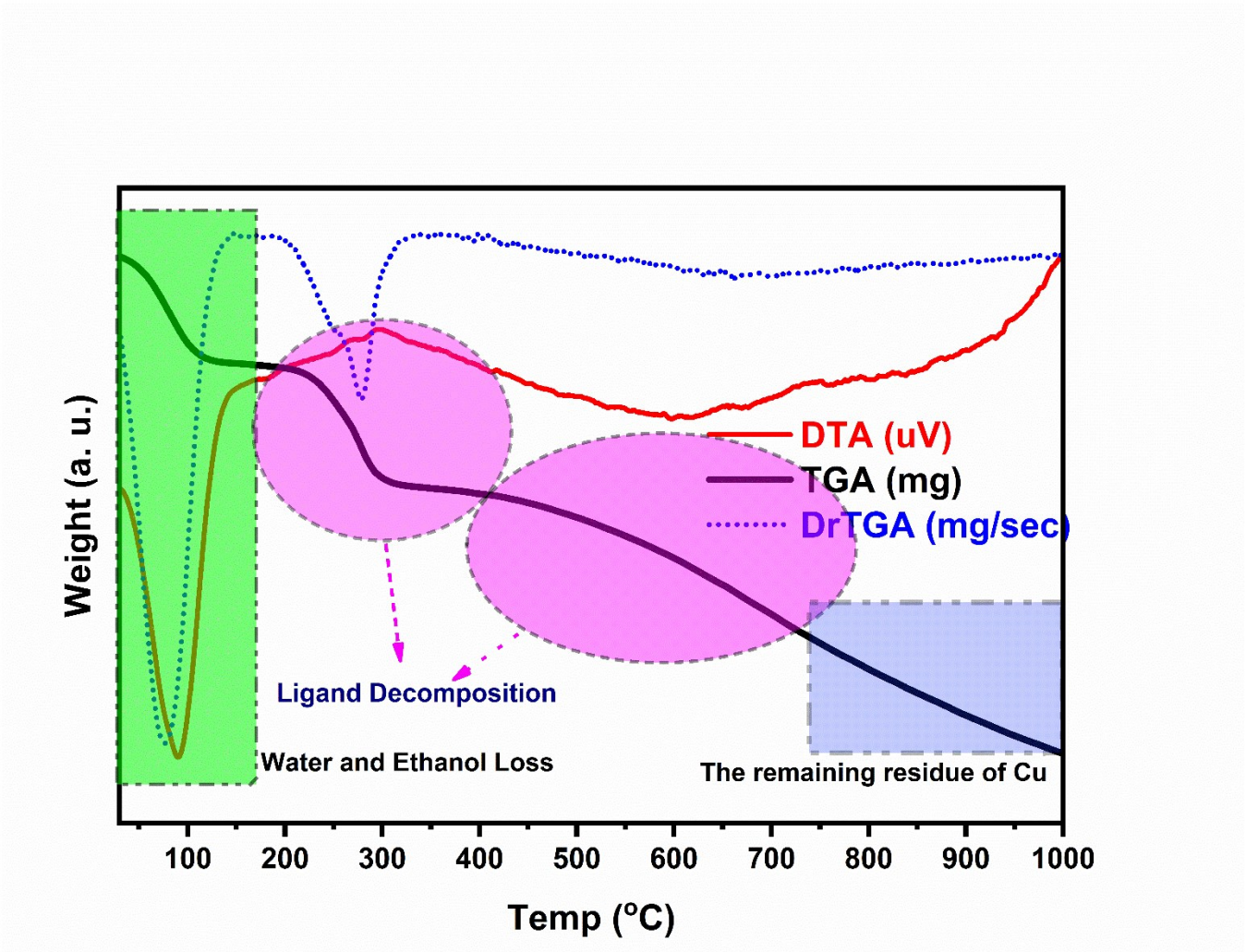

Fig. S12: The thermogravimetric analysis (TGA-DTGA) of the N1.

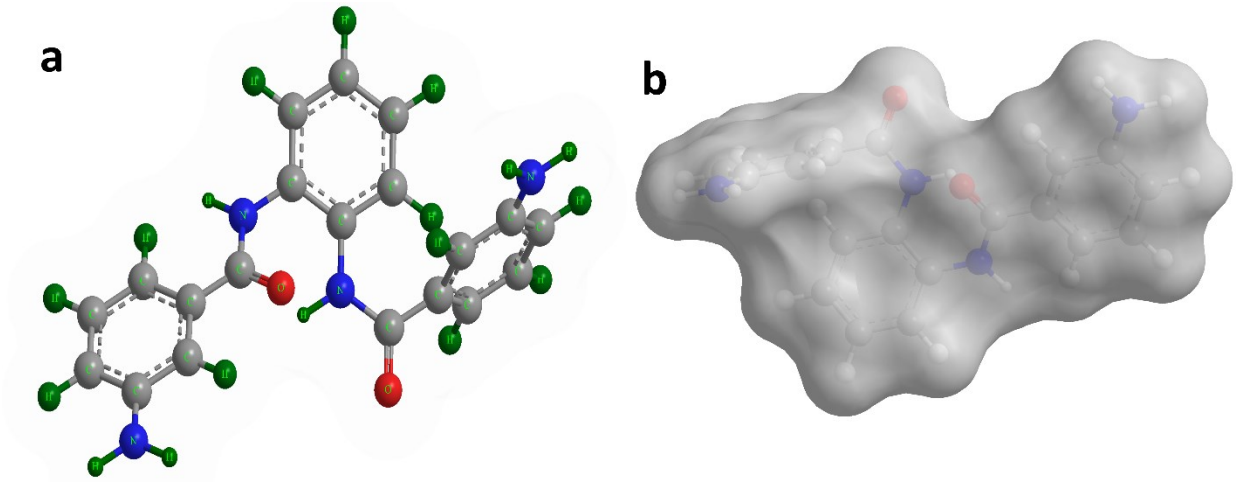

Fig. S13: [a] 3D Structural, and **[b]** advanced molecular surface representation of the Schiff base ligand **(A1).**

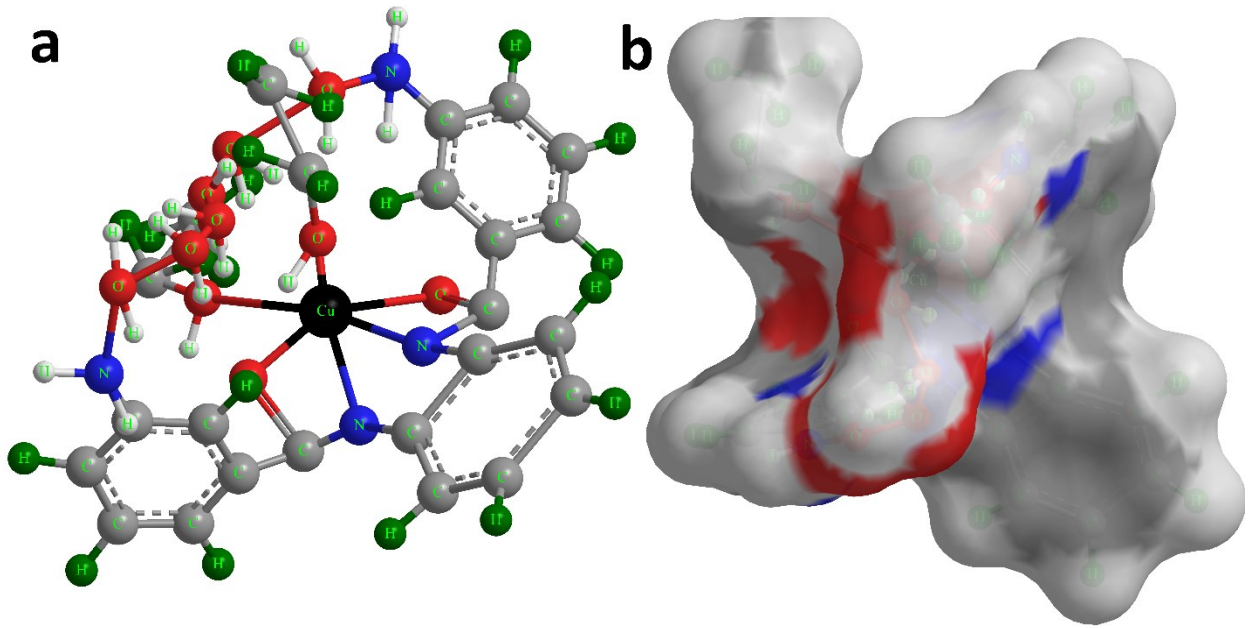

Fig. S14: [a] 3D Structural, and **[b]** advanced molecular surface representation of the nano copper complex **(N1)**

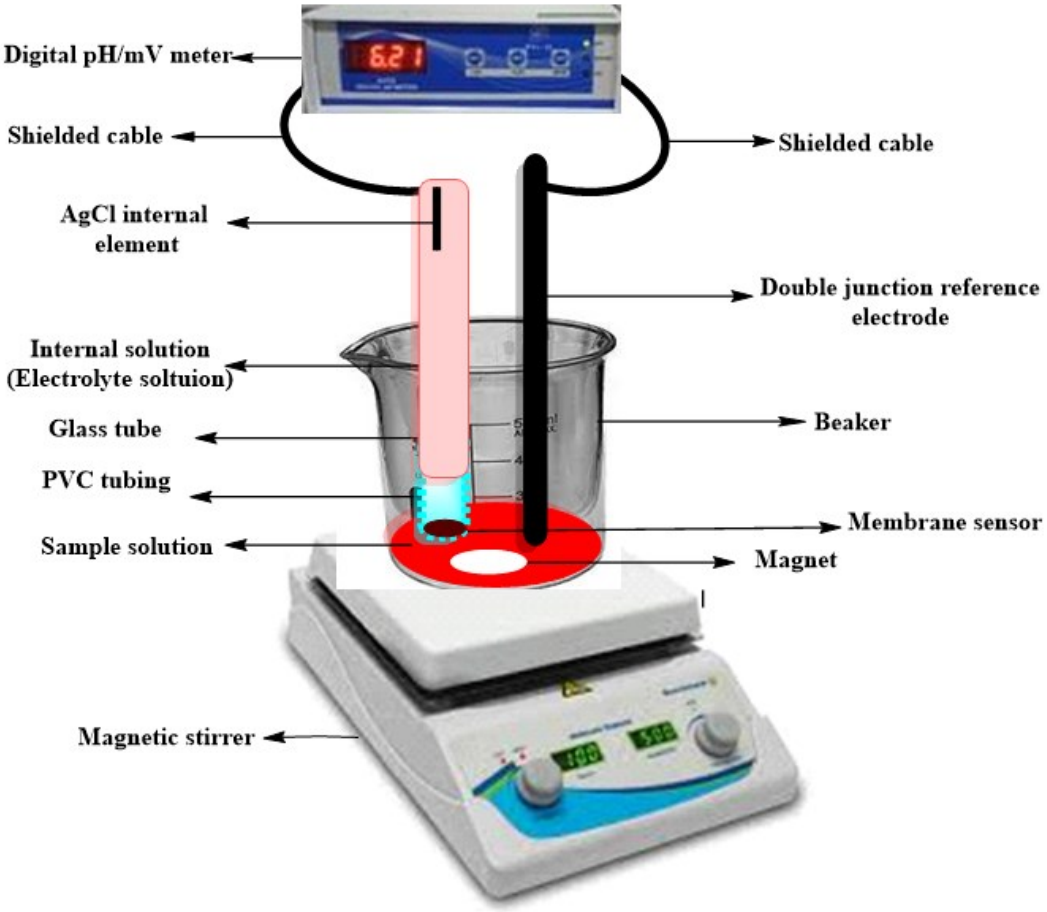

Fig. S15. Schematic diagram of the electrochemical cell for potentiometric measurements.

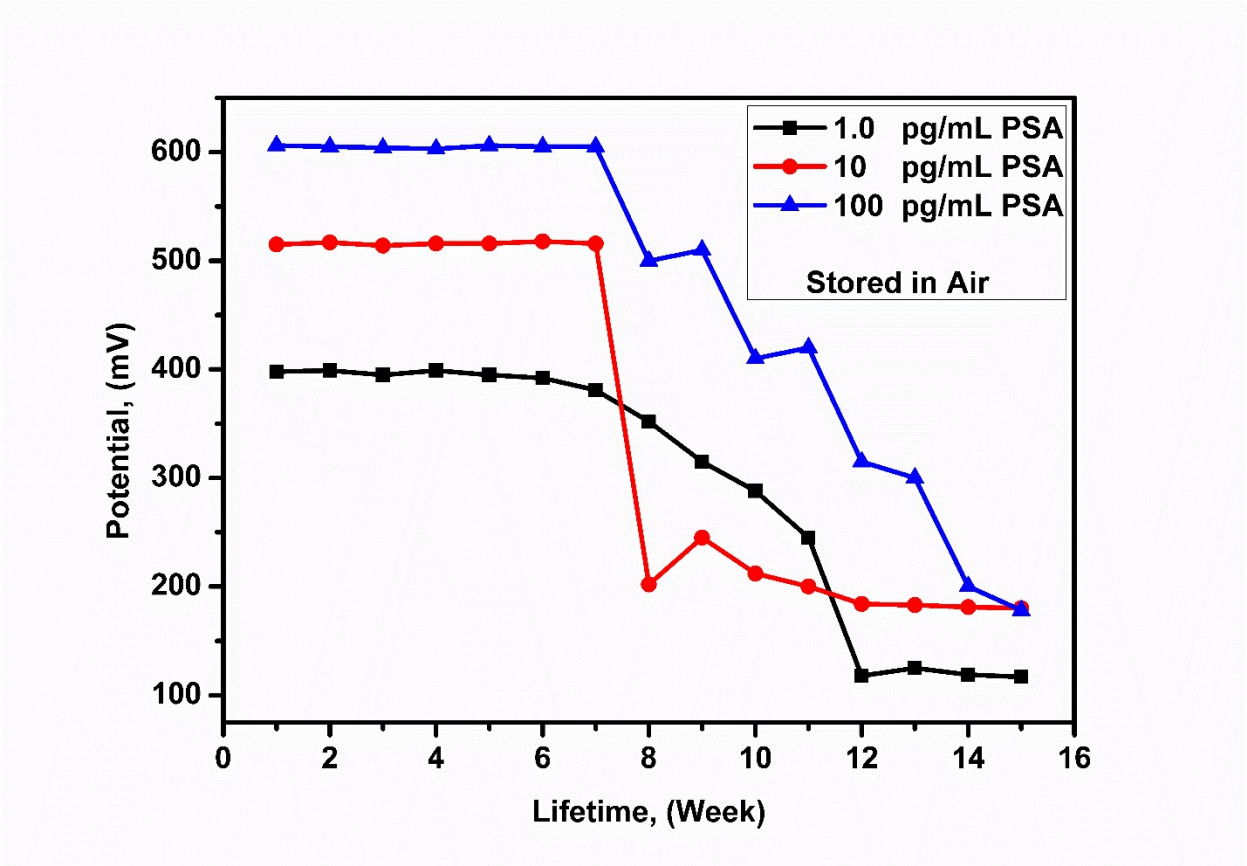

Fig. S16: The N1@PVC electrode lifetime performance stored in air.

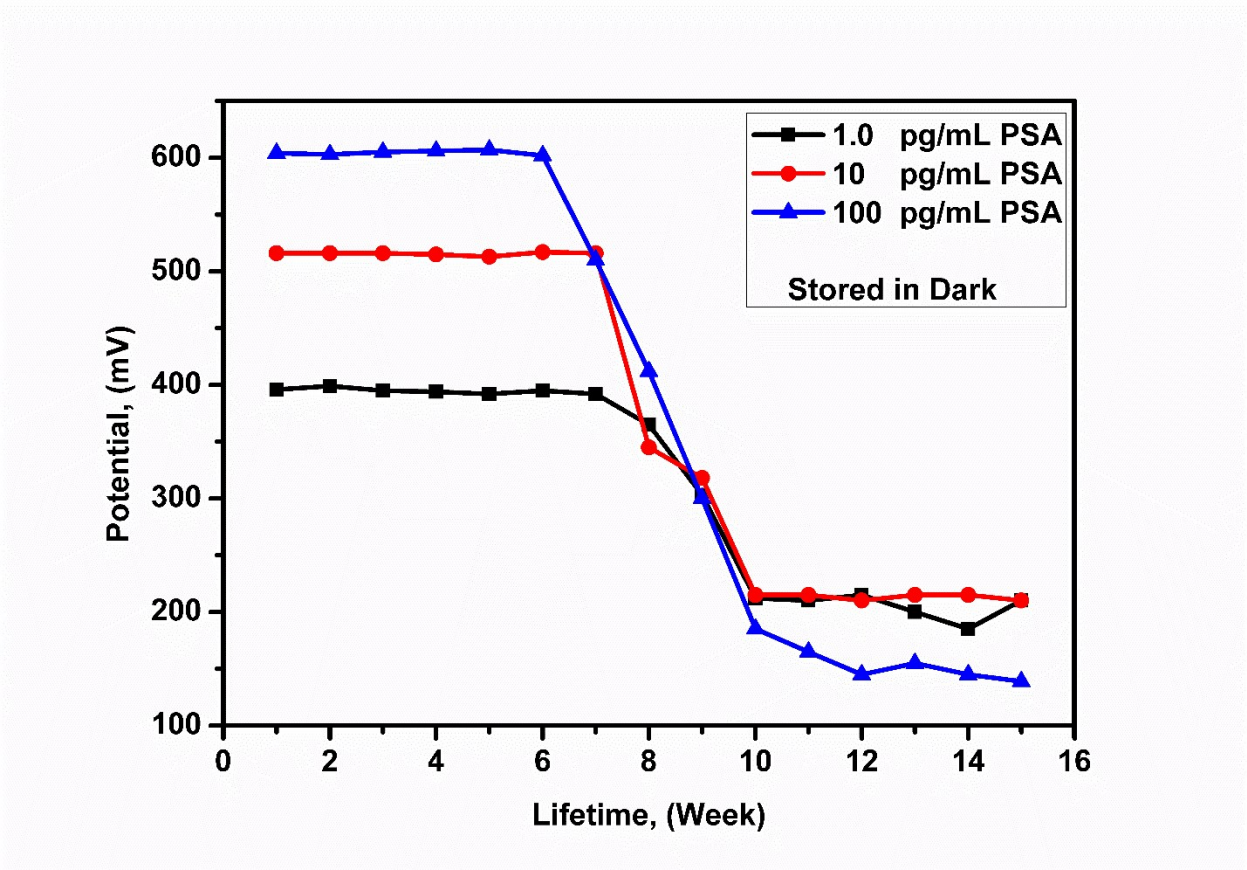

Fig. S17: The N1@PVC electrode lifetime performance stored in dark.

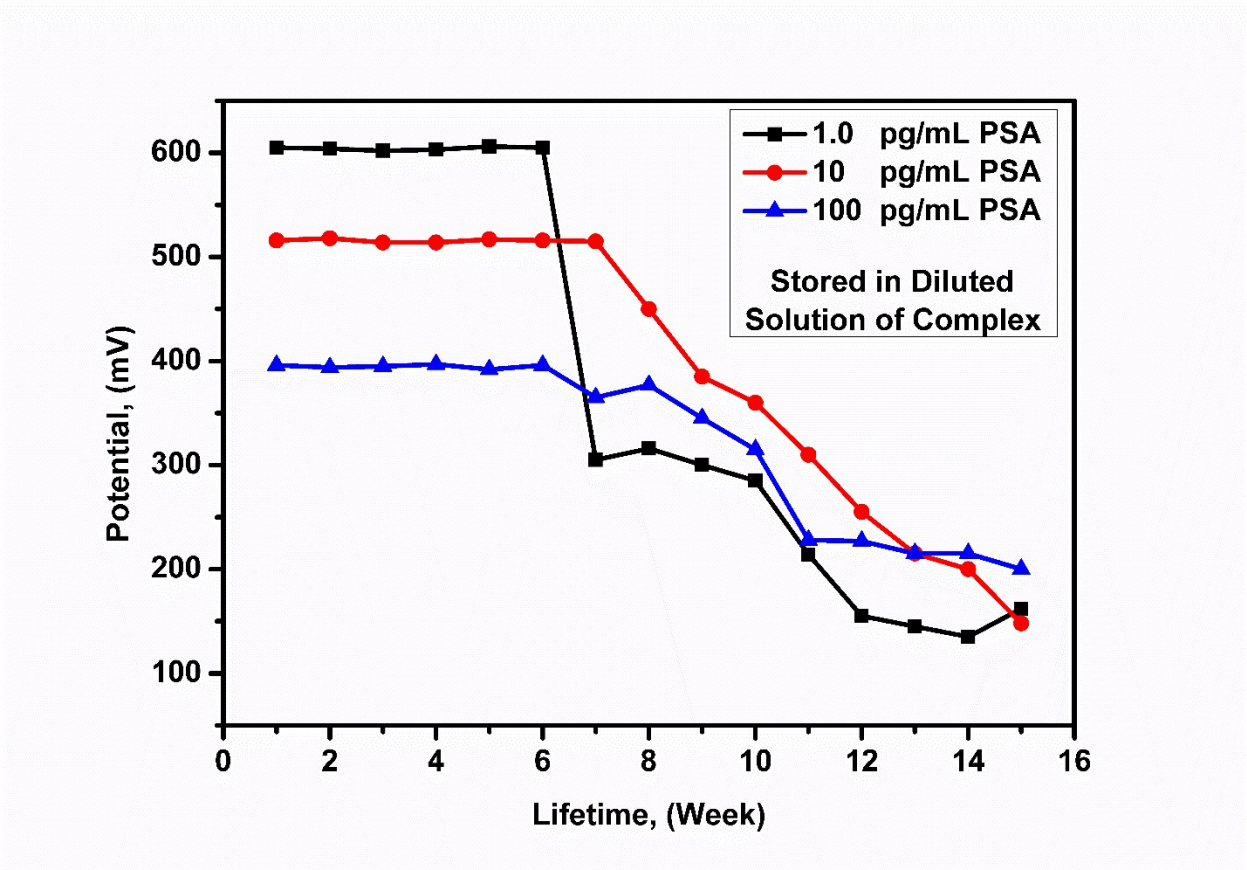

Fig. S18: The N1@PVC electrode lifetime performance stored in diluted solution of N1.

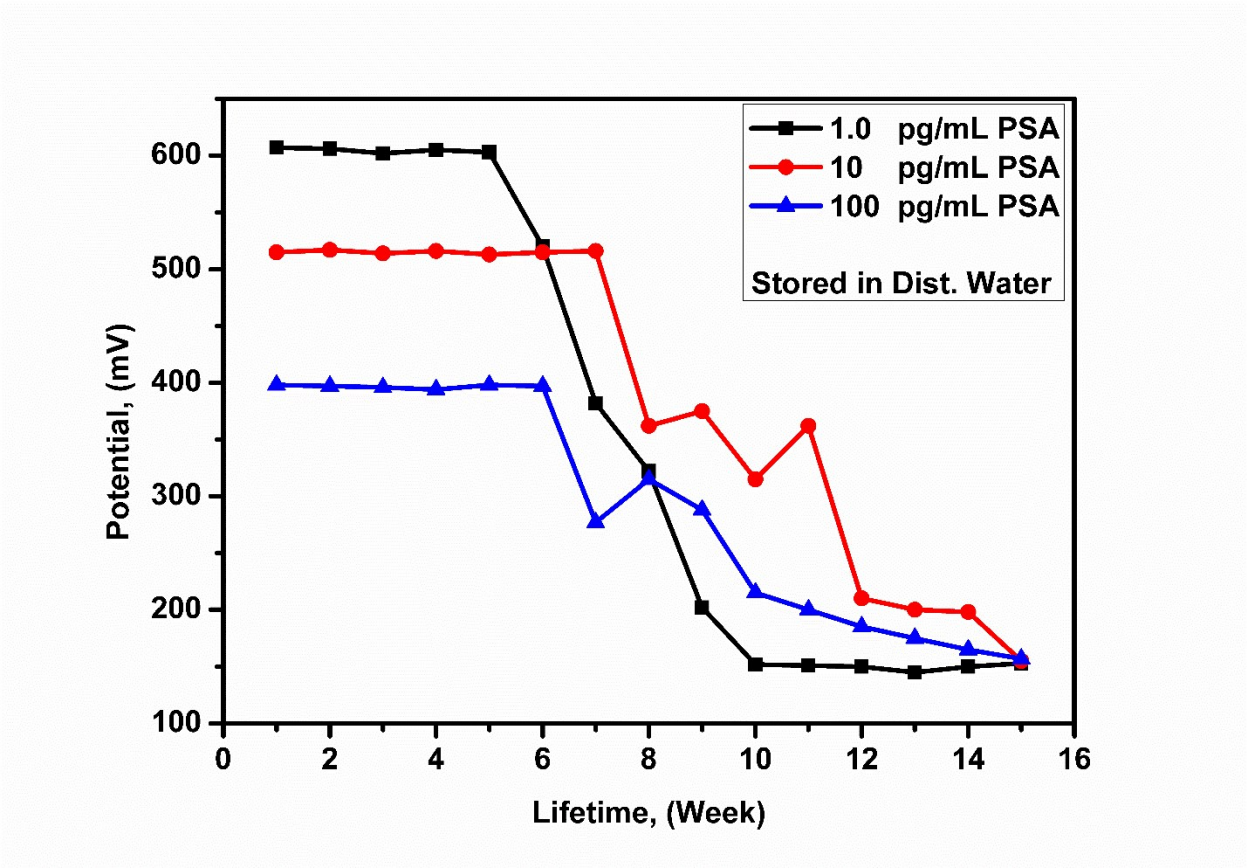

Fig. S19: The N1@PVC electrode lifetime performance stored in distilled water.

Table S1. Analytical and some important physical measurements for A1 and N1

Assignments		A1	N1
Preparation Method		Reflux	Reflux
Color		Reddish brown	Dark green
Aspect		Powder	Fine crystal
Melting Point (°C)		174.1	> 300
Reaction Time		2 days	2 days
Yield (%)		96.5	82.1
Chemical Formula		$C_{24}H_{30}N_4O_4$	$C_{24}H_{40}CuN_4O_{10}$
Molecular Weight(g/mol)		438.53	608.15
Elemental analysis (Calc.)/ Found	**C %**	(65.73)/ 65.94	(47.40)/ 47.19
	H %	(6.90)/ 6.73	(6.63)/ 6.92
	N %	(12.78)/ 12.89	(9.21)/ 9.18
Characteristic infrared frequencies (cm^{-1})	**ν(OH)-ν(NH) azo-hydrazine form**	3635-3278	3631-3275
	ν(NH_2)		
	υ(CH)-sp^3	2935	2921
	ν(C=O) -ν(C=N) - ν(C=C)	1730-1440	1733-1445
	ν(C-N)	1385	1353
	ν(Cu–O)	---	522
	ν(Cu–N)	---	436
UV- λ_{max} (nm)		226, 296, 440	246, 300, 345, 424

Table S2: EDX analysis of the A1 and N1.

Material	Element	Weight %	Atomic %	Net Int.	Error %
A1	C	65.53	71.75	135.93	9.73
	N	12.67	11.95	2.80	1.14
	O	21.80	16.30	29.41	5.06
N1	C	47.68	60.30	78.86	8.72
	N	9.43	10.23	6.00	4.92
	O	32.40	26.86	25.07	11.29
	Cu	10.49	2.61	30.45	3.74

Table S3: Response characteristics of electrode utilizing various solvent mediators

Solvent mediator	Linear concentration range	Slope/mV per decade
DOP	5.0 fg/mL – 10.0 ng/mL	29.26 ± 0.87
DOS	40.0 fg/mL – 5.0 ng/mL	24.2 ± 1.86

Table S4: Selectivity coefficients $K_{A,B}^{pot}$ for various interfering analytes using separate solution method.

Interfering analyte	**Potential reading (mV)**	$K_{A,B}^{pot}$
CEA	235	7.89×10^{-4}
AFP	222	7.62×10^{-4}
CK-T	182	6.90×10^{-4}
CK-MB	195	7.12×10^{-4}
Star	156	6.50×10^{-4}
Cit	215	7.48×10^{-4}
Glu	165	6.63×10^{-4}
Lac	158	6.53×10^{-4}
Bio	185	6.95×10^{-4}
Bil	192	7.07×10^{-4}
Chol	166	6.65×10^{-4}
Trig	163	6.60×10^{-4}
Caff	168	6.68×10^{-4}

Table S5: Evaluation of intra-day, inter-day accuracy, precision, and results of recovery study using spiking technique.

Standard PSA Added, *	**Repeatability Intra-day precision**				**Reproducibility Inter-day precision**				**PSA recovery (Percent ± SD)**	
	X	SD	CV	RE%	X	SD	CV	RE%	Intra-day	Inter-day
10.0 fg/mL	9.704	0.241	0.058	1.031	9.874	0.634	0.402	1.013	97.04 ± 0.24	98.74 ± 0.63
100 fg/mL	97.49	3.763	14.16	1.026	96.59	0.393	0.155	1.035	97.49 ± 3.76	96.59 ± 0.39
50.0 pg/mL	49.57	1.862	3.466	1.009	48.05	0.434	0.188	1.041	99.15 ± 1.86	96.10 ± 0.43
500 pg/mL	499.6	2.414	5.826	1.001	499.1	1.825	3.331	1.002	99.92 ± 2.41	99.82 ± 1.83

* Each reading was repeated three times; X, mean values; SD, standard deviation; CV, the coefficient of variation; %RE, percent of relative error.

Table S6: Comparison between the nano Cu(II)-complex biosensor and some existing methods for the determination of PSA.

Method	Linear detection range	LOD	Reference
Colorimetric aptasensor	0.1–100 ng/mL	20.0 pg/mL	(2)
Colorimetric bioassay based on a switchable linker	10–35 µg/mL/	0.1 pg/mL	(7)
Immunosensor based on Au-NPs @ multienzyme-particle electrodes	1.0- 40 ng/mL	0.5 pg/mL	(8)
Au-upconversion nanoparticles	0.04×10^{-18} -1×10^{-18} M	0.032×10^{-18} M	(9)
Fluorometric aptamer-based assay	0.05–150 pg/mL	0.043 pg/mL	(10)
Electrochemiluminescence (ECL)	0.001-100 ng/mL	0.44 pg/mL	(11)
Electro chemiluminescent immunosensor	0.001–80 ng/mL	0.30 pg/mL	(13)
Voltammetry immunosensing platform	0.75–100.0 ng/mL	0.27 ng/mL	(14)
Impedimetric immunosensor	0.01–100 and 1–20000 ng/mL	5.4 pg/mL	(15)
Photoelectrochemical immunosensor	0.01–500 ng/mL	5 pg/mL	(16)
Photoelectrochemical immunosensor	0.02 pg/mL-200 ng/mL	6.8 fg/mL	(17)
Cooperated signal amplification strategy	0.001-10000 ng/mL	0.03 pg/mL	(18)
Chemiluminescence resonance energy transfer (CRET)	1.0-100 ng/mL	0.6 ng/mL	(22)
Sandwich-type electrochemical immunosensor	1.0 pg/mL- 100 ng/mL	0.45 pg/mL	(23)
Nano Cu(II) complex biosensor	0.005-10000 pg/mL	0.297 pg/mL	The present work

Table S7: Determination of PSA in serum real samples using nano Cu(II)-complex biosensor and compared the results with rapid tests, and ELISA standard method.

Sample	Spiked PSA (pg/mL)	Found, (pg/mL)			SD	CV	RE%
		ELISA standard method for PSA detection*	Average potential reading (mV)**	Corresponding average amount of PSA found, **			
Serum samples	0.01	0.011	277.5	0.01	0.022	0.003	1.038
	5.0	5.14	484.2	4.953	0.18	0.032	1.01
	50.0	49.85	571.4	49.33	0.783	0.613	1.014
	100.0	102.3	603.2	97.15	0.992	0.984	1.029
	1000	1009.6	668.1	999.7	1.315	2.99	1

* The mean values were performed with official standard method (Enzyme-linked immunosorbent assay for the quantitative determination of PSA; **Each reading was repeated three times; SD, standard deviation; CV, coefficient of variation; RE%, relative error percent.

Materials

All the solvents and chemicals used in this paper were of analytical reagent grade and were used without purification. Polyvinyl chloride powder PVC of high molecular weight, dioctyl phthalate (DOP), and dioctyl sebacate (DOS), tetrahydrofuran (THF) of purity greater than 99 %. 1,2-phenylenediamine($C_6H_8N_2$), 3-aminobenzoic acid ($C_7H_7NO_2$) and copper(II) chloride hydrated $CuCl_2.2H_2O$; were obtained from Sigma Aldrich. Standard prostate-specific antigen (PSA) of different buffered concentrations were supplied by Monobind, USA.

Instruments

The characterization and applications were performed using different analytical techniques: The mass spectra of solid **A1** and **N1** were recorded using a Thermo Scientific-ISQ single quadrupole mass spectrometer. The ^{1}H-NMR spectra of samples in deuterated dimethyl sulfoxide (DMSO-D^6) were performed with a 500 MHz NMR spectrometer (JEOL-ECA 500II). Elemental analysis (C-H-N) were performed using a Costech ECS-4010- analyzer. The Fourier transform-infrared (FT-IR) spectra were recorded with a JASCO FT/IR-460 spectrophotometer with use of KBr tablets in the range from 400 to 4000 cm^{-1} at room temperature. Ultra Violet Visible (UV–Vis) spectra were gained for the prepared Schiff base ligand (**A1**) and copper complex (**N1**) by using a PerkinElmer 550 spectrophotometer in 1 cm quartz cell in ethanol; over a range of 200–900 nm. The FE-SEM images and EDX spectroscopy spectra were recorded with a combination of field emission scanning electron microscopy (FE-SEM), and element mapping by spatially resolved energy-dispersive X-ray spectroscopy (EDX) (JEOL JSM-6510LV advanced electron microscope with a LAB-6 cathode at 520 keV). The structure of the formed phases was examined by using a high-resolution transmission electron microscope (HR-TEM) with an acceleration voltage up to 200 kV (TEM, JEOL-JEM-2100, Tokyo, Japan). Thermal analysis (DSC/TGA) of the samples were evaluated with a Shimadzu thermogravimetric analyser TGA50, Germany with a rate of 10 °C min^{-1} in nitrogen atmosphere. All potentiometric measurements were performed at room temperature with constant magnetic stirring, with an Orion Model A720 digital pH/mV meter and an Orion Ross Combination pH electrode (Model 81-02) for all pH measurements. Copper complex-PVC based electrode was used for all potentiometric measurements in conjunction with a double junction reference electrode (Orion Model 90-02) containing KNO_3 (10% w/v) in

the outer compartment\silver-silver chloride reference electrode. The data were analysed with Origin-8. The structures, 3D geometrical structures and Schemes were drawn using "ChemBioDraw Ultra12" program.